

From Non-interacting to Interacting Picture of Quark Gluon Plasma in presence of a magnetic field and its fluid property

Jayanta Dey¹, Sarthak Satapathy¹, Ankita Mishra², Souvik Paul³,
Sabyasachi Ghosh¹

¹Indian Institute of Technology Bhilai, GEC Campus, Sejbahar, Raipur 492015, Chhattisgarh, India

² Department of Mechanical Engineering, Guru Ghasidas University, Bilaspur 495009, India

³ Department of Physical Sciences, Indian Institute of Science Education and Research Kolkata, Mohanpur, West Bengal 741246, India

Abstract

We have attempted to build a parametric based simplified and analytical model to map the interaction of quarks and gluons in presence of magnetic field, which has been constrained by quark condensate and thermodynamical quantities like pressure, energy density etc., obtained from the calculation of lattice quantum chromodynamics. To fulfill that mapping, we have assumed a parametric temperature and magnetic field dependent degeneracy factor, average energy, momentum and velocity of quarks and gluons. Implementing this QCD interaction in calculation of transport coefficient at finite magnetic field, we have noticed that magnetic field and interaction both are two dominating sources, for which the values of transport coefficients can be reduced. Though the methodology is not so robust, but with the help of its simple parametric expressions, one can get a quick rough estimation of any phenomenological quantity, influenced by temperature and magnetic field dependent QCD interaction.

1 Introduction

Extremely strong magnetic fields have been known to exist during the electroweak phase transition of the universe as suggested by cosmological models [1]. Large values of magnetic fields are also present in the interior of dense neutron stars called magnetars [2]. Studying quantum field theory in the presence of magnetic field has led to many interesting observations such as magnetic catalysis [3], chiral magnetic effect [4], inverse magnetic catalysis [5, 6] and many more. These phenomena might be indirectly observed in the laboratories of heavy ion collision (HIC) experiments like RHIC and LHC, where an approximately $m_\pi^2 - 10m_\pi^2$ magnetic field is expected to be produced after collision due to two opposite heavy-ionic currents [7]. Refs. [8, 9, 10] have addressed a possible space time evolution of electromagnetic fields, produced in the laboratories of HIC experiments. Refs. [11, 12, 13, 14] (also relevant references therein) have studied on evolution picture of expanding tiny medium in presence of magnetic field through the equations of magneto hydrodynamic (MHD). Impact of external magnetic field through transport simulation can be noticed in Ref. [15]. Dissipative picture of MHD or transport simulation need a field dependent transport coefficients inputs and therefore, a parallel microscopic calculation of transport coefficients in present of magnetic field [16] is an important topic in the community of heavy ion physics. The transport coefficients in presence of

magnetic field are recently investigated in Refs. [17, 18, 19, 20, 21, 22, 23, 24, 25, 26, 27, 28, 29, 30, 31, 32, 33, 34, 35, 36, 37, 38, 39, 40, 41, 42, 43, 44, 45, 46, 47, 48, 49, 50], where field impact in shear viscosity [17, 18, 19, 20, 21, 22, 23, 24, 25, 26], electrical conductivity [27, 28, 29, 30, 31, 32, 33, 34, 35, 36, 37, 38, 39, 40, 41, 42, 43], bulk viscosity [44, 45, 46, 47, 48] for light quark sector as well as heavy quark sector [49, 50] are investigated. Present article has gone through similar directional investigation.

With respect earlier works, present work has a unique combination of two components. One is the mapping of QCD interaction at finite temperature and magnetic field via fitting QCD thermodynamic, provided by recent lattice quantum chromodynamics (LQCD) calculations [5, 6]. Another is a detail multi-component anatomy of shear viscosity and electrical conductivity of quark gluon plasma in presence of magnetic field, which has been considered for that interacting picture. Without field picture, we can find a long list of Refs. [51, 52, 53, 54, 55, 56, 57, 58, 59, 60, 61] and references therein, where a temperature dependent QCD interaction is mapped but that much investigations are not found for magnetic field picture. After the LQCD results of thermodynamics in presence of magnetic field [5, 6], a revised effort from effective QCD model calculation [62, 63, 64, 65] have been attempted. In this context, present work has attempted to find a simple parametric mapping of LQCD thermodynamics in presence of magnetic field [5, 6].

In earlier Ref. [66] by Satapathy et al., an attempt is made for building a simplified parametric model through matching the LQCD thermodynamics without magnetic field. There, a temperature dependent degeneracy factor of QGP system is prescribed to map the temperature dependent QCD interaction. Extending the earlier study of Ref. [66], a quasi-particle model at finite magnetic field picture is attempted in present article, where a temperature and magnetic field dependent degeneracy factor is first proposed by matching the LQCD thermodynamics in presence of magnetic field [5, 6], then they are used for estimating anisotropic components of transport coefficients of QGP.

The article is organized as follows. Next in Sec. (2), the mapping of LQCD thermodynamics in presence of magnetic field has been addressed. After developing the quasi particle description, it is applied to estimate transport coefficients like shear viscosity and electrical conductivity at finite magnetic field in Sec. (3), whose framework is briefly addressed in Sec. (5) with two subsections - (5.1) and (5.2). At the end in Sec. (4) we have summarized our investigations.

2 Mapping LQCD Thermodynamics at finite magnetic field

Owing to the basic statistical mechanics, pressure P , number density n and energy density ϵ of grand canonical ensemble at finite temperature $T = 1/\beta$ and zero chemical potential ($\mu = 0$) can be obtained from its partition function Z and their final expressions are respectively

$$\begin{aligned} P &= \frac{T}{V} \ln Z \\ &= g \frac{T}{a} \int \frac{d^3 k}{(2\pi)^3} \ln\{1 + ae^{-\beta E}\} \\ &= g \int \frac{d^3 k}{(2\pi)^3} \left[\frac{k^2}{3E} \right] \frac{1}{e^{\beta E} + a}, \end{aligned} \tag{1}$$

$$n = g \int \frac{d^3 k}{(2\pi)^3} \left[1 \right] \frac{1}{e^{\beta E} + a}, \tag{2}$$

$$\epsilon = g \int \frac{d^3 k}{(2\pi)^3} \left[E \right] \frac{1}{e^{\beta E} + a}, \tag{3}$$

where g is degeneracy factor, and $a = \pm 1$ for Fermion and Boson medium.

Using above equations for massless quark gluon plasma (QGP) system, we will get:

$$\begin{aligned} P_{QGP} &= g_g \int \frac{d^3k}{(2\pi)^3} \left[\frac{k^2}{3E} \right] \frac{1}{e^{\beta E} - 1} + g_Q \int \frac{d^3k}{(2\pi)^3} \left[\frac{k^2}{3E} \right] \frac{1}{e^{\beta E} + 1} \\ &= \left[g_g + g_Q \left(\frac{7}{8} \right) \right] \frac{\zeta(4)}{\pi^2} T^4 = \left[g_g + g_Q \left(\frac{7}{8} \right) \right] \frac{\pi^2}{90} T^4 \approx 5.2 T^4, \end{aligned} \quad (4)$$

$$\begin{aligned} n_{QGP} &= g_g \int \frac{d^3k}{(2\pi)^3} \left[1 \right] \frac{1}{e^{\beta E} - 1} + g_Q \int \frac{d^3k}{(2\pi)^3} \left[1 \right] \frac{1}{e^{\beta E} + 1} \\ &= n_g + n_Q = \left[g_g + g_Q \left(\frac{3}{4} \right) \right] \frac{\zeta(3)}{\pi^2} T^3 \approx 5.23 T^3, \end{aligned} \quad (5)$$

$$\begin{aligned} \epsilon_{QGP} &= g_g \int \frac{d^3k}{(2\pi)^3} \left[E \right] \frac{1}{e^{\beta E} - 1} + g_Q \int \frac{d^3k}{(2\pi)^3} \left[E \right] \frac{1}{e^{\beta E} + 1} \\ &= \left[g_g + g_Q \left(\frac{7}{8} \right) \right] \frac{3\zeta(4)}{\pi^2} T^4 = \left[g_g + g_Q \left(\frac{7}{8} \right) \right] \frac{3\pi^2}{90} T^4 \approx 15.6 T^4, \end{aligned} \quad (6)$$

where $g_g = 16$ and $g_Q = 36$ are degeneracy factors of gluons and 3-flavor quarks. Here n_{QGP} stands for total number density of QGP, which is different from net quark density (which is zero at zero quark chemical potential). Massless values of entropy density s_{QGP} can also be obtained as

$$s_{QGP} = \frac{\epsilon + P}{T} = \frac{4P}{T} \approx 20.8 T^3. \quad (7)$$

If we calculate average energy or momentum of massless Boson and Fermion medium, then we will get

$$\begin{aligned} E_{av}^{g,Q}(m=0) &= k_{av}^{g,Q}(m=0) = \frac{\int \frac{d^3p}{(2\pi)^3} \frac{E}{e^{\beta E+a}}}{\int \frac{d^3p}{(2\pi)^3} \frac{1}{e^{\beta E+a}}} \\ &= 3T \frac{\zeta(4)}{\zeta(3)} \text{ for gluon or, } a = -1, \\ &= \frac{7T}{2} \frac{\zeta(4)}{\zeta(3)} \text{ for quark or, } a = +1, \\ &= 3T \text{ for spinless parton or, } a = 0. \end{aligned} \quad (8)$$

Using those average values, one can rewrite P_{QGP} , ϵ_{QGP} in terms of n_{QGP} as:

$$\begin{aligned} P_{QGP} &= \left[\frac{k_{av}^2(m=0)}{3E_{av}(m=0)} \right]_g n_g + \left[\frac{k_{av}^2(m=0)}{3E_{av}(m=0)} \right]_Q n_Q \\ &= \left[\frac{k_{av}(m=0)}{3} \right]_g n_g + \left[\frac{k_{av}(m=0)}{3} \right]_Q n_Q \\ &= \left[T \frac{\zeta(4)}{\zeta(3)} \right] g_g \frac{\zeta(3)}{\pi^2} T^3 + \left[\frac{7T}{6} \frac{\zeta(4)}{\zeta(3)} \right] g_Q \left(\frac{3}{4} \right) \frac{\zeta(3)}{\pi^2} T^3 \\ &= \left[g_g + g_Q \left(\frac{7}{8} \right) \right] \frac{\pi^2}{90} T^4 \approx 5.2 T^4, \end{aligned} \quad (9)$$

$$\epsilon_{QGP} = \left[E_{av}(m=0) \right]_g n_g + \left[E_{av}(m=0) \right]_Q n_Q,$$

$$\begin{aligned}
&= \left[3T \frac{\zeta(4)}{\zeta(3)} \right] g_g \frac{\zeta(3)}{\pi^2} T^3 + \left[\frac{7T}{2} \frac{\zeta(4)}{\zeta(3)} \right] g_Q \left(\frac{3}{4} \right) \frac{\zeta(3)}{\pi^2} T^3 \\
&= \left[g_g + g_Q \left(\frac{7}{8} \right) \right] \frac{3\pi^2}{90} T^4 \approx 15.6 T^4 .
\end{aligned} \tag{10}$$

In more simplified way, by considering average energy of spinless parton ($a=0$), we can write:

$$\begin{aligned}
P_{QGP} &= \left[\frac{k_{\text{av}}(m=0)}{3} \right] \times n_{QGP} = \left[\frac{3T}{3} \right] \times 5.23T^3 \approx 5.23T^4 \\
\epsilon_{QGP} &= \left[E_{\text{av}}(m=0) \right] \times n_{QGP} = \left[3T \right] \times 5.23T^3 \approx 15.69T^4 .
\end{aligned} \tag{11}$$

Reader may notice very negligible difference between Eq. (11) and Eqs. (9), (10), so considering average energy and momentum of massless and spinless parton as $3T$ might not be too bad assumption to consider.

High T quantum chromo dynamics (QCD) matter might behave like this and these massless values are popularly known as Stefan Boltzmann (SB) limits. It is lattice QCD (LQCD), who provide us a better picture thermodynamical quantities like P , ϵ , s etc. As we go from high to low T range, a reduced values of thermodynamical quantities with respect their SB limits are observed in LQCD picture. There are different quasi-particle type frameworks [51, 52, 53, 54, 55, 56, 57, 58, 59, 60, 61] (see also references therein) have been attempted to map the reduced values of LQCD thermodynamics. In this context, we have tried to map this fact as a reduction of degeneracy factors. If we go below quark-hadron transition temperature (T_c), then we will get hadronic matter (HM), where hadrons are the relevant degrees of freedom of the system. If we assume that pion and kaon as most abundant mesons, made by u, d and s quarks, then for a quick estimations, one can calculate their massless expressions of thermodynamical quantities:

$$\begin{aligned}
P_{HM} &= (g_\pi + g_K) \int \frac{d^3k}{(2\pi)^3} \left[\frac{k^2}{3E} \right] \frac{1}{e^{\beta E} - 1} = (g_\pi + g_K) \frac{\zeta(4)}{\pi^2} T^4 \approx 0.76 T^4 , \\
n_{HM} &= (g_\pi + g_K) \int \frac{d^3k}{(2\pi)^3} \left[1 \right] \frac{1}{e^{\beta E} - 1} = (g_\pi + g_K) \frac{\zeta(3)}{\pi^2} T^3 \approx 0.77 T^3 , \\
\epsilon_{HM} &= (g_\pi + g_K) \int \frac{d^3k}{(2\pi)^3} \left[E \right] \frac{1}{e^{\beta E} - 1} = (g_\pi + g_K) \frac{3\pi^2}{90} T^4 \approx 2.28 T^4 , \\
s_{HM} &= \frac{\epsilon_{HM} + P_{HM}}{T} = (g_\pi + g_K) \frac{4\zeta(4)}{\pi^2} T^3 \approx 3.04 T^3 ,
\end{aligned} \tag{12}$$

where $g_\pi = 3$, $g_K = 4$ are degeneracy factors of π and K mesons respectively. Now if we see the Lattice quantum chromodynamics (LQCD) data of $P(T)$, $\epsilon(T)$, $s(T)$, which is copied from Ref. [6] and pasted in Fig. 2(a), then one can notice that the data points are located within the ranges $0.76 < \frac{P}{T^4} < 5.2$, $2.28 < \frac{\epsilon}{T^4} < 15.6$, $3.04 < \frac{s}{T^4} < 20.8$. In this context, quark-hadron phase transition may be considered as transition between two massless values of thermodynamical quantities for QGP to HM system, which can be realized as reduction of degeneracy factor from $\left[g_g + g_Q \left(\frac{7}{8} \right) \right] \approx 47.5$ to $(g_\pi + g_K) \approx 7$. Hence, one can understand the smooth cross-over transition from QGP to HM phase through smooth reduction of degeneracy factors of QGP system. To execute this idea, temperature dependent fraction/factor $g(T)$ has to be first multiplied with thermodynamical quantities, given in Eq. (6) and then by matching LQCD data, one can get the parametric form of $g(T)$. Hence, $g(T) = 1$ will correspond to non-interacting picture or (roughly) massless case or SB limits of QGP, given in Eqs. (6). While we will get interacting QGP when we use parametric form of $g(T)$, which will be always less than one in entire temperature range. Refs. [5, 6] have provided P_{LQCD} and

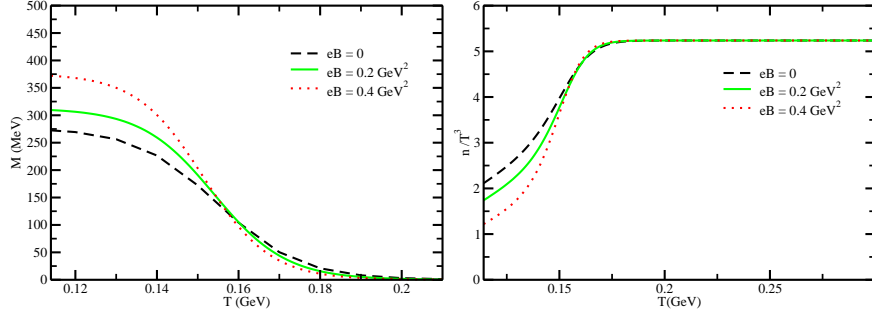


Figure 1: Constituent quark mass M (left) and normalized total number density n_{LQCD}/T^3 vs temperature T at different magnetic field. The estimations are based on LQCD quark condensate data [5].

ϵ_{LQCD} data but not n_{LQCD} data. Using their quark condensate ($\langle\bar{q}q\rangle_T$) data, we can go with rough estimate of constitute quark mass as $M \approx \frac{M_N}{3}\langle\bar{q}q\rangle_T$, with nucleon mass $M_N = 0.940$ GeV. Reader can recognize the idea is guided from gap equation of NJL model with zero current quark mass. Then using that $M(T)$, we can estimate total number density. Let us called it as n_{LQCD} and can be estimated by using the expressions:

$$n_{LQCD} = g_g \int \frac{d^3k}{(2\pi)^3} \frac{1}{e^{\beta k} - 1} + g_Q \int \frac{d^3k}{(2\pi)^3} \frac{1}{e^{\beta\sqrt{k^2+M^2(T)}} + 1}. \quad (13)$$

The $M(T)$ (left) and $n_{LQCD}(T)$ (right) are shown by black dash line in Fig. (1). Now we have searched $g(T)$, which satisfy

$$n_{LQCD} = g(T) \times n_{QGP} = g(T) \times 5.23T^3. \quad (14)$$

Using that $g(T)$, we can get a rough estimation of pressure, energy density and entropy density as $g(T) \times P_{QGP} = g(T) \times 5.2T^4$, $g(T) \times \epsilon_{QGP} = g(T) \times 15.6T^4$ and $g(T) \times s_{QGP} = g(T) \times 20.8T^3$ respectively, whose qualitative reduction trend is found as expected but they are quite far from the actual LQCD data values - P_{LQCD} , ϵ_{LQCD} and s_{LQCD} . The dotted, dash and dash-dotted lines in left-upper panel of Fig. (2) has explored this fact. We notice that they are far from LQCD data, given by circles, dimonds and squares.

Now, matching all LQCD thermodynamical quantities through a single parameter tuning is probably an impossible task, therefore more than one parameter can be helpful. So along with $g(T)$, if we consider E_{av} , k_{av} as other tuning parameters, which might be deviated from massless expressions, given in Eq. (8), we may get better fitted picture. Similar to the T dependent fraction/factor $g(T)$, we can assume $f_E(T)$ and $f_k(T)$ can be multiplied with massless and spinless values of average energy and momentum as

$$\begin{aligned} E_{av}(T) &= 3T \times f_E(T) \\ k_{av}(T) &= 3T \times f_k(T), \end{aligned} \quad (15)$$

where using standard relativistic relation among momentum, velocity and energy -

$$k_{av}(T) = v_{av}(T) \times E_{av}(T), \quad (16)$$

we can get a connection between average velocity $v_{\text{av}}(T)$, $f_E(T)$ and $f_k(T)$ as

$$f_k(T) = f_E(T) \times v_{\text{av}}(T) . \quad (17)$$

One can get $f_E = 1$, $f_k = 1$ and $v_{\text{av}}(T) = 1$ for massless case. Now we can tune our $f_E(T)$ and $v_{\text{av}}(T)$ by fitting LQCD data of P_{LQCD} and ϵ_{LQCD} by imposing simplified quasi-particle relations:

$$\begin{aligned} \epsilon_{LQCD} &= [E_{\text{av}}] n_{LQCD} \\ &\approx f_E(T) \times g(T) \times 15.69T^4 \\ P_{LQCD} &= \left[\frac{k_{\text{av}}(T)v_{\text{av}}(T)}{3} \right] n_{LQCD} \\ &\approx v_{\text{av}}^2(T) \times f_E(T) \times g(T) \times 5.23T^4 \end{aligned} \quad (18)$$

Let us try to understand an overall idea of our proposed tuning set up. First we have attempted to map T -dependent quark condensate, which is in general mapped by constituent quark mass in effective QCD models but here we did it in different way. We first build number density data by using T dependent quark mass, then imposing that still the total number density is basically number density of massless QGP, where their degeneracy factor mainly modified. So indirectly degeneracy factor carry the information of T -dependent quark condensate instead of constituent quark mass. Since number density is simply integration of thermal distribution, so we have use it as reference quantity to extract the temperature profile of tuning parameter - degeneracy factor. Just by multiplying T -dependent degeneracy factor with number density of massless QGP, one may get its corresponding values in interacting picture. Now for other thermodynamical quantities like pressure, energy density, which are roughly average values of energy and $\frac{1}{3} \times \text{momentum} \times \text{velocity}$, multiplied by number density. Here we are assuming those average quantities, related with one-body kinematics will also be deviated from its massless limits as it happens for degeneracy factors. Hence by tuning the degeneracy factor first we are able to map quark condensate information of LQCD and next by tuning the average kinematics of spinless partons, we can manage to map the LQCD thermodynamics.

In presence of magnetic field along z -axis, we can get an anisotropy in pressure but if we consider pressure along z -direction (P_z), then thermodynamics relation

$$s = \frac{\epsilon + P_z}{T} \quad (19)$$

remain same [5]. So, earlier expressions can be used for finite B picture by tuning T , B dependent parameters $g(T, B)$, $f_E(T, B)$, $f_k(T, B)$ or $v_{\text{av}}(T, B)$. Hence, T and B dependent LQCD thermodynamics [5, 6] can be realized via simple parametric relations:

$$\begin{aligned} n_{LQCD}(T, B) &= g(T, B) \times 5.23T^3 \\ \epsilon_{LQCD}(T, B) &= E_{\text{av}}(T, B) \times n_{LQCD}(T, B) \\ &= f_E(T, B) \times g(T, B) \times 15.69T^4 \\ P_{LQCD}(T, B) &= \frac{v_{\text{av}}^2(T, B) \times E_{\text{av}}(T, B)}{3} \times n_{LQCD}(T, B) \\ &= v_{\text{av}}^2(T, B) \times f_E(T, B) \times g(T, B) \times 5.23T^4 . \end{aligned} \quad (20)$$

The fitted curves of LQCD data and the T , B dependent tuning parameters $g(T, B)$, $E_{\text{av}}(T, B)$, $k_{\text{av}}(T, B)$ and $v_{\text{av}}(T, B)$ are shown in Figs. (2).

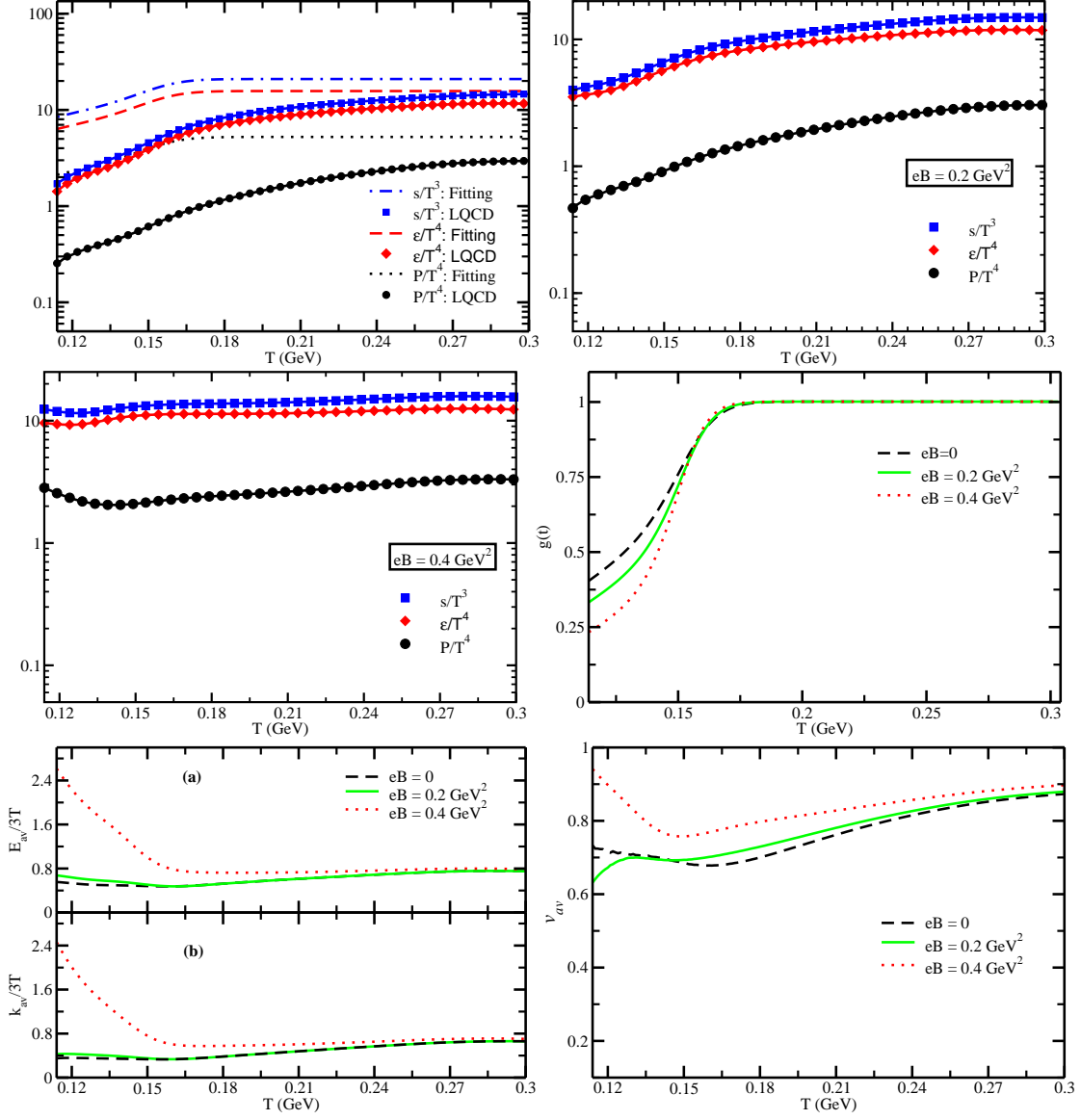


Figure 2: LQCD data of pressure (black circles), energy density (red diamonds) and entropy density (blue squares) are fitted at $eB = 0$ (Left-upper panel), $eB = 0.2 \text{ GeV}^2$ (Right-upper panel), $eB = 0.4 \text{ GeV}^2$ (Left-middle panel) by our proposed model (solid curves) with tuning parameters degeneracy factor $g(T, B)$ (Right-middle panel), average energy $E_{av}(T, B)$, momentum $k_{av}(T, B)$ (Left-lower panel) and velocity $v_{av}(T, B)$ (Right-lower panel). Using only $g(T)$ tuning parameter, dotted, dash and dash-dotted lines in left-upper panel are showing the deviation from LQCD data points, which is resolved by other tuning parameters.

At the end of this section, let us briefly touch the well known inverse magnetic catalysis (IMC) effect, which was the key points of recent LQCD data [5, 6]. The fact is as follows. The chiral condensate $\langle \bar{q}q \rangle_T$ in absence of magnetic field melts down near transition temperature T_c , when one goes from hadronic to quark temperature domain. In presence of magnetic field enhancement of condensate was very well known phenomena and known as magnetic catalysis (MC). LQCD data [5, 6] at low T show this MC but near transition temperature an IMC effect is noticed. Constituent quark mass $M(T, B)$, as shown in left panel of Fig. (1), is revealing that fact as it is proportionally mapped from condensate $\langle \bar{q}q \rangle_T(T, B)$. Further temperature derivative of mass or condensate we can get peak at T_c , which will be shifted towards lower values as we increase B . This reduction of T_c with B become well known graphical representation of IMC phenomena. However, in thermodynamical quantities like pressure, energy density, entropy density and transport coefficients like shear viscosity and electrical conductivity, this IMC fact becomes faint due thermal distribution ($\sim e^{-\beta M(T, B)}$). So searching effect of IMC might be tedious job from those quantities (addressed in present article). However, interaction measure $\epsilon - 3P$ and its connected transport coefficients like bulk viscosity (as $\zeta \propto (\epsilon - 3P)$) might able to expose the IMC pattern, where their peak might be shifted with eB .

2.1 Picture of reducing degeneracy factor

To visualize the possibility of reduction degeneracy factor with decreasing temperature, let us recapitulate the similar fact of reducing degrees of freedom in di-atomic or n-atomic molecular system. At low temperature, di-atomic or n-atomic molecules have $3 \times 2 - 1$ or $3 \times n - k$ degrees of freedoms, because it carries 1 or k number of atomic bindings. This bonding can be broken at high temperature and its degrees of freedom can be increased from $3 \times 2 - 1 = 5$ to $3 \times 2 = 6$ or from $3 \times n - k$ to $3 \times n$. Based on the equipartition theorem, (internal) energy density of di-atomic or n-atomic molecular system will be proportional to its degrees of freedom, therefore internal energy or other thermodynamical quantities like pressure, entropy will be enhanced with increasing temperature. Similarly, when we go from hadronic phase (assuming abundant $\pi + K$ mesons) to QGP (u, d, s quarks and gluons) by increasing temperature, the degeneracy factor probably transform smoothly from $g = 7$ to $g = 52$.

Formulating actual mechanism of this fact might be very difficult (but certainly a good problem of QCD sector), but it can be visualize by counting quantum states of any hadron and its constituent's quantum states. For example, a colorless π^+ state in the low T or hadronic phase can be melted into three color u and three anti-color \bar{d} in high T or QGP phase. So a transition from 1 to 6 quantum states in color space can be realized (extending static to dynamical picture, one can add color gluons also). Similar to color space, when we include flavor/iso-spin, spin spaces, we will get a collective reduction of degeneracy factor from $g = 52$ to $g \approx 7$ by decreasing the temperature from QGP to hadronic phase. Reduction of LQCD thermodynamics from their SB limits can be realized by the reduction of degeneracy factor of QGP system. So $g(T)$ can grossly map T -dependent QCD interaction.

Now, the temperature basically measure of randomness of the system. So, low to high T represents less to more quantum states, interpreting less to more randomness. On the other hand, magnetic field plays opposite role as it tries to make the system be more ordered. So low to high eB represents less to more orderliness or more to less randomness. Owing to that fact, low T and high eB corresponds to hadronic phase with smaller number of degeneracy factors, while, high T and low eB corresponds to QGP phase with larger number of degeneracy factors. Reduction of transition temperature T_c by increasing eB is noticed in LQCD data [5, 6], which can classify two domains in T - eB plane. In right-middle panel of Fig. (2), reducing of degeneracy factors by increasing eB in low T domain can be noticed. Roughly within $0.1 \text{ GeV} < T < 0.170 \text{ GeV}$ and $0 < eB < 0.4 \text{ GeV}^2$,

major suppression of degeneracy factors is occurred by decreasing T and increasing eB . In this way, $g(T, B)$ can grossly map QCD interaction as a function of T and eB .

3 Estimation of shear viscosity and electrical conductivity of interacting QGP in presence of magnetic field

In this section, we will see the role of QCD interaction in presence of magnetic field on transport coefficients like shear viscosity and electrical conductivity, where the interaction is mapped by quasi-particle description, discussed earlier section. The details formalism of shear viscosity and electrical conductivity in presence of magnetic field are derived in Appendix, given in Sec. (5).

In absence of magnetic field, medium follow isotropic transport properties, for which we will get single component of shear viscosity (η) and electrical conductivity (σ), but they become multi-component in presence of magnetic field. We will get five shear viscosity components η_n ($n = 0, 1, \dots, 4$) and three electrical conductivity components σ_n ($n = 0, 1, 2$), which can be classified into three main components - parallel ($\eta_{\parallel}, \sigma_{\parallel}$), perpendicular ($\eta_{\perp}, \sigma_{\perp}$) and Hall ($\eta_{\times}, \sigma_{\times}$) components. Getting guided from Sec. (5) (Appendix), let us first write the expressions of η and σ for massless QGP system in absence of magnetic field:

$$\begin{aligned}\eta &= \frac{\beta}{15}g_g \int \frac{d^3\vec{k}}{(2\pi)^3} \frac{\vec{k}^4}{E^2} \tau_c f_0(1+f_0) + \frac{g_Q\beta}{15} \int \frac{d^3\vec{k}}{(2\pi)^3} \frac{\vec{k}^4}{E^2} \tau_c f_0(1-f_0) \\ &= \left[g_g + \frac{7}{8}g_Q \right] \frac{4\tau_c \zeta(4)T^4}{5\pi^2}\end{aligned}\quad (21)$$

and

$$\begin{aligned}\sigma &= \frac{g_Q}{3} \sum_{f=u,d,s} \frac{\tilde{e}_f^2 \beta}{3} \int \frac{d^3\vec{k}}{(2\pi)^3} \frac{\vec{k}^2}{E^2} \tau_c f_0(1-f_0) \\ &= \frac{g_Q}{3} \sum_{f=u,d,s} \tilde{e}_f^2 \frac{\zeta(2)}{3\pi^2} \tau_c T^2\end{aligned}\quad (22)$$

For more simplified case - spinless and massless QGP system (by considering MB distribution function), Above expressions can be written as

$$\eta = \left[g_g + g_Q \right] \frac{4\tau_c T^4}{5\pi^2}\quad (23)$$

$$\sigma = \frac{g_Q}{3} \sum_{f=u,d,s} \tilde{e}_f^2 \frac{1}{3\pi^2} \tau_c T^2 .\quad (24)$$

Applying quasi-particle description in Eqs. (23), (24), we can express η and σ as

$$\begin{aligned}\eta &= \frac{\tau_c}{15}(g_g + g_Q)\beta \int \frac{d^3\vec{k}}{(2\pi)^3} \left(\frac{\vec{k}}{E}\right)^2 \vec{k}^2 f_0 \\ &\approx \frac{v_{av}^2 k_{av}^2}{15} \tau_c \chi \\ \sigma &= \frac{g_Q}{3} \sum_{f=u,d,s} \frac{\tilde{e}_f^2 \tau_c}{3} \beta \int \frac{d^3\vec{k}}{(2\pi)^3} \left(\frac{\vec{k}}{E}\right)^2 f_0\end{aligned}\quad (25)$$

$$\approx \sum_{f=u,d,s} \frac{\tilde{e}_f^2 \tau_c}{3} v_{\text{av}}^2 \chi_e. \quad (26)$$

where different static susceptibilities can be expressed in terms of their massless values as

$$\begin{aligned} \chi &= g(T) \times \chi(m=0) \\ \chi_e &= g(T) \times \chi_e(m=0) \end{aligned} \quad (27)$$

with

$$\begin{aligned} \chi(m=0) &= \left(\frac{\partial n}{\partial \mu} \right)_{\mu=0} = (g_g + g_Q) \beta \int \frac{d^3 \vec{k}}{(2\pi)^3} f_0 = (g_g + g_Q) \frac{T^2}{\pi^2} \\ \chi_e(m=0) &= \frac{g_Q}{3} \beta \int \frac{d^3 \vec{k}}{(2\pi)^3} f_0 = \frac{g_Q}{3} \frac{T^2}{\pi^2}. \end{aligned} \quad (28)$$

We can roughly get back massless Eqs. (23), (24) from quasi-particle Eqs. (25), (26) by putting $v_{\text{av}} = 1$, $k_{\text{av}} = E_{\text{av}} = 3T$. So we can build a simple analytic expressions of η and σ in quasi-particle picture:

$$\begin{aligned} \eta &= \left[v_{\text{av}}^2(T) f_k^2(T) g(T) \right] (g_g + g_Q) \frac{9T^4}{15\pi^2} \tau_c \\ \sigma &= \left[v_{\text{av}}^2(T) g(T) \right] g_Q \frac{T^2}{9\pi^2} \tau_c \sum_{f=u,d,s} q_f^2, \end{aligned} \quad (29)$$

where the quantities inside the third bracket mainly sources of quasi-particle description, for which estimation will be modified from massless values. This modification basically map the QCD interaction, hidden in LQCD thermodynamics.

Now let us go for finite B picture. From Sec. (5), realizing the anatomy of parallel and perpendicular components of viscosity and conductivities of charged medium,

$$\begin{aligned} \eta_{\parallel} &= \frac{\eta}{1 + 4(\tau_c/\tau_B)^2} \\ \eta_{\perp} &= \frac{\eta}{1 + (\tau_c/\tau_B)^2} \\ \sigma_{\parallel} &= \sigma \\ \sigma_{\perp} &= \frac{\sigma}{1 + (\tau_c/\tau_B)^2}, \end{aligned} \quad (30)$$

we can build quasi-particle expressions of QGP system:

$$\begin{aligned} \eta_{\parallel}(T, B) &= \left[v_{\text{av}}^2(T, B) f_k^2(T, B) g(T, B) \right] \frac{9T^4}{15\pi^2} \tau_c \left[g_g + \frac{g_Q}{3} \sum_{f=u,d,s} \frac{1}{1 + 4(\tau_c/\tau_{B,f})^2} \right] \\ \eta_{\perp}(T, B) &= \left[v_{\text{av}}^2(T, B) f_k^2(T, B) g(T, B) \right] \frac{9T^4}{15\pi^2} \tau_c \left[g_g + \frac{g_Q}{3} \sum_{f=u,d,s} \frac{1}{1 + (\tau_c/\tau_{B,f})^2} \right] \\ \sigma_{\parallel}(T, B) &= \left[v_{\text{av}}^2(T) g(T) \right] g_Q \frac{T^2}{9\pi^2} \tau_c \sum_{f=u,d,s} q_f^2 \\ \sigma_{\perp}(T, B) &= \left[v_{\text{av}}^2(T) g(T) \right] g_Q \frac{T^2}{9\pi^2} \tau_c \sum_{f=u,d,s} q_f^2 \frac{1}{1 + (\tau_c/\tau_{B,f})^2}, \end{aligned} \quad (31)$$

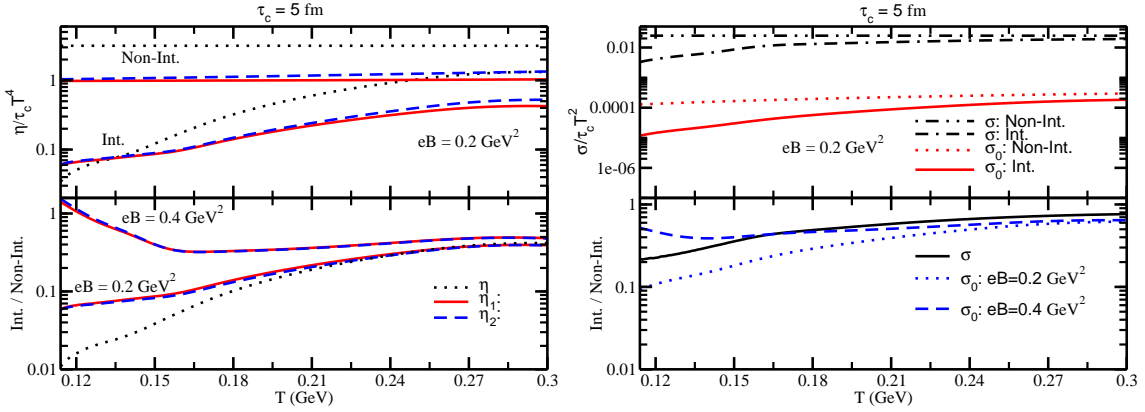


Figure 3: Left-upper: T dependence of η (dotted line), $\eta_1(eB = 0.2\text{GeV}^2)$ (solid line) and $\eta_2(eB = 0.2\text{GeV}^2)$ (dash line) for their non-interacting and interacting cases. Left-lower: Ratio of interaction to non-interaction values of η , η_1 and η_2 at different magnetic fields. Right-upper: T dependence of σ , $\sigma_0(eB = 0.2\text{GeV}^2)$ for their non-interacting and interacting cases. Right-lower: Ratio of interaction to non-interaction values of σ , σ_0 at different magnetic fields.

where $\tau_{B,f} = \frac{E_{av}}{q_f B}$ is inverse of synchrotron frequency of different flavor f with electric charge q_f .

Let us come to the numerical estimation. According to Eqs. (25), (22) or (23), (24), the normalized value $\eta/(\tau_c T^4)$ and $\sigma/(\tau_c T^2)$ for massless QGP will be constant as shown by straight horizontal dotted (Left-upper) and dash double-dotted (Right-upper) lines in Fig. (3). Next, using Eq. (29), we will get the values of $\eta/(\tau_c T^4)$ (black dotted line) and $\sigma/(\tau_c T^2)$ (red dotted line) of interacting QGP, which are suppressed from their massless values and also carry an additional T -dependent profile due to the quasi-particle T -dependent quantities - $v_{av}(T)$, $f_k(T)$ and $g(T)$. The results say that similar to reduced profile of thermodynamical quantities along T -axis with respect to their massless or SB limits, transport coefficients will also follow that pattern and the reduction of both quantities increase as one goes high T or perturbative QCD domain to low T or non-perturbative QCD domain. Here, the dissipation information of transport coefficients, hidden in relaxation time τ_c , are normalized to reveal their non-interaction and interaction component of thermodynamical phase space only. Unlike to thermodynamical quantities, transport coefficients basically carry two parts of interactions - one is in thermodynamical phase-space via quasi-particle based tuning parameters and another is in relaxation time, interpreting dissipation component of interaction. A possible connection between two interaction is attempted in Ref. [66], where two time scale, coming from thermodynamics and dissipation interactions are compared. Searching the connection between two interactions might be difficult and framework dependent. Hence, without entering to this complicated part, we have take two interactions as two independent components, where former is guided from LQCD data and latter is kept as free by choosing free parameter τ_c . The term ‘‘non-interacting’’ might be little misleading term. Non-interacting dissipation mean $\tau_c \rightarrow \infty$, where transport coefficients are diverged but non-interacting thermodynamical phase-space provide a massless expression. So terms non-interacting and interacting in present article will not applicable for dissipation component, rather only for thermodynamical phase-space component. In both cases (interacting and non-interacting), we will keep relaxation time as finite and free parameter.

By taking ratio of interaction to non-interaction values, as shown in lower panels of Fig. (3), we can see that when we go from $T = 0.300$ GeV to 0.120 GeV, shear viscosity and electrical

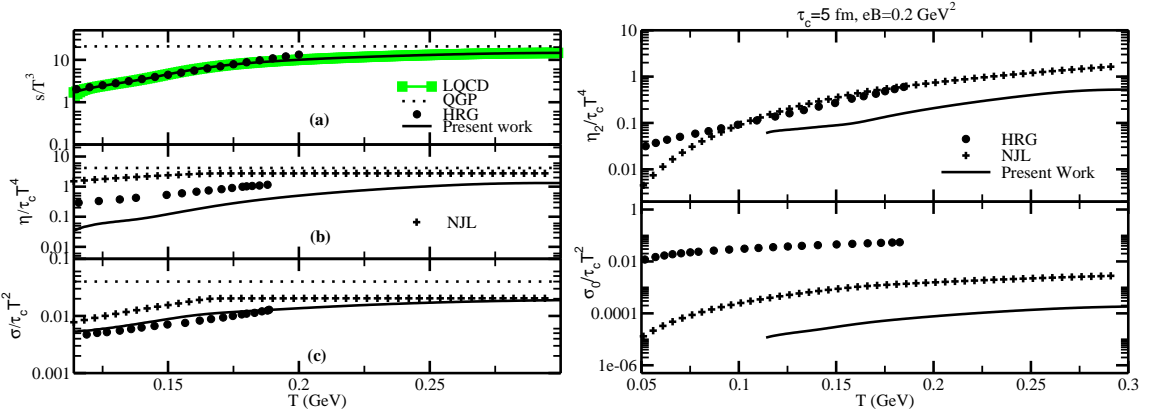


Figure 4: Left: Comparing our estimation (black solid line) of entropy density (upper panel), shear viscosity (middle panel) and electrical conductivity (lower panel) with the corresponding values of (ideal) HRG model [23], NJL model [38, 21] and massless limits (dotted line). Green squares are LQCD data [6] of entropy density. Right: perpendicular components of shear viscosity (upper panel) and electrical conductivity (lower panel) in our model, HRG model [23], NJL model [38, 21] at $eB = 0.2 \text{ GeV}^2$ and $\tau_c = 5 \text{ fm}$.

conductivity can respectively face 50% to 98.5% and 30% to 90% reduction due to interaction.

Now, at finite B picture, non-interacting results η_1 (red solid line), η_2 (blue dash line) and σ_0 (red dotted line) are shown in upper panels of Fig. (3), which shows a reduction with respect to their without field results. One can understand that this reduction comes through the $\tau_B \approx \frac{3T}{q_f B}$, which transform τ_c to a reduced scale $\frac{\tau_c}{1 + \left(\frac{\tau_c}{\tau_B}\right)^2}$ roughly. The reduction will increase with increasing of B

and decreasing of T . Going to interaction picture at finite B , we will get further modification and we have to use now T and B -dependent quantities - $v_{av}(T, B)$, $f_k(T, B)$ and $g(T, B)$. The results are shown by red solid, blue dash lines for η_1, η_2 in left-upper panel of Fig. (3) and by red solid line for σ_o in right-upper panel of Fig. (3). So finite magnetic field will first change the values of transport coefficients via $\tau_B(T, B)$ and then interaction will change their values further through $v_{av}(T, B)$, $f_k(T, B)$ and $g(T, B)$. The T, B dependence of interaction can be visualized better way in lower panels of Fig. (3), which reveal a less reduction in low T and high B domain due to interaction as observed in thermodynamical quantities also. Another point - anisotropy in dissipation can be realized through the inequality parallel $>$ perpendicular component - $\eta_1 > \eta_2$ and $\sigma > \sigma_0$.

3.1 Comparing interaction strength with earlier estimations

In this section, we will try to explore how close/far our estimation of transport coefficients with other model-dependent estimations, which can map the interaction of LQCD thermodynamics. In Fig. (4), left-upper panel shows that the LQCD data [6] (green squares), our fitted curve (black solid line) and (ideal) HRG model estimation [23] (black circles) for s/T^3 at $eB = 0$ are well agreement. Extracting the interaction information from LQCD thermodynamics via quasi-particle T -dependent quantities $v_{av}(T)$, $f_k(T)$ and $g(T)$, we have basically projecting them to transport coefficients. We have compared our estimations of $\eta/(\tau_c T^4)$ and $\sigma/(\tau_c T^2)$ with HRG [23] (circles) and NJL [38, 21] (pluses) model estimations in middle and lower panels of Fig. (4). All results are

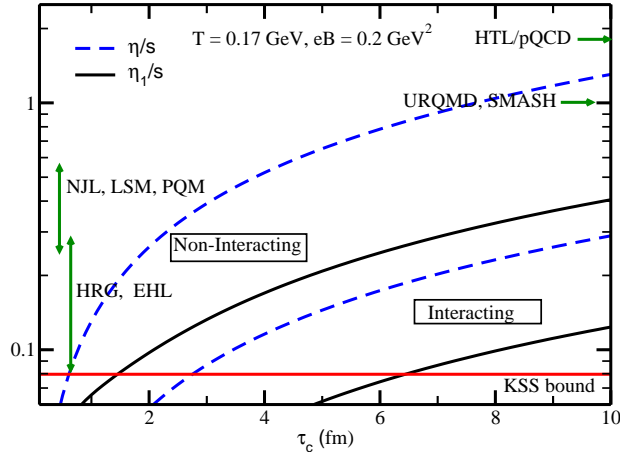


Figure 5: Viscosities to entropy density ratio for non-interacting and interacting QGP at $eB=0$ (dash line), $eB = 0.2 \text{ GeV}^2$ (solid line). Green arrows for earlier estimations at $eB = 0$.

suppressed from their SB or massless limits, shown by dotted horizontal line. Suppression values of s/T^3 , $\eta/(\tau_c T^4)$ and $\sigma/(\tau_c T^2)$ are mapping their non-pQCD estimations. Qualitative trends of different models are quite similar with little quantitative differences in transport coefficients. At finite B , these quantitative differences are revealing more as shown in the right panel of Fig. (2). From Ref. [6], we notice that finite B extension of s in HRG model is not well matched with corresponding LQCD values, which is also true from NJL model estimations of Refs. [65, 38]. In that context our estimations is purely projected from LQCD thermodynamics in presence of magnetic field. So T , B dependence of our estimated transport coefficients might carry more accurate T , B dependent non-perturbative QCD interaction.

Let us now focus on famous dimensionless quantity - ratio between shear viscosity and entropy density, which measure the fluid nature of the medium. From experimental side, this quantity should be very close to KSS bound $1/(4\pi)$ [67], which is drawn by red solid (horizontal) line in Fig. (5). At $B = 0$ case, a long list of references can be found on the estimations of η/s , where few [68, 69, 70, 71, 72, 73, 74, 75, 76, 78, 79, 80, 81, 82] are tabulated in Table [1]. Relaxation time τ_c are calculated in different models and they get order of magnitude of η/s but in present article, we keep it as parameter. By plotting η/s against τ_c -axis for non-interacting and interacting case, we can get an effective τ_c ranges, within which earlier estimated values are located. One can find that pQCD [68] and box-simulation [75, 76] based on URQMD [75], SMASH [76] codes are showing 10-20 larger values than KSS bound. Whereas effective QCD models [69, 70, 71, 72, 73, 74] like NJL [69, 70, 71, 72], LSM [73], QM [74] models addressed an intermediate ranges $\eta/s \approx 2.5 - 5.5$ (marked by green arrow). Effective hadron Lagrangian (EHL) models as well as HRG models provide the range $\eta/s \approx 2.5 - 0.08$ (marked by green arrow), where K-matrix HRG model provide KSS values 0.08 near transition temperature $T \approx 0.170 \text{ GeV}$. After realizing the range of η/s within 1-20 times KSS bound can be found for $\tau_c \approx 0.5 - 10 \text{ fm}$, we have shown their finite B extended results at $eB = 0.2 \text{ GeV}^2$. Due to log scale of η/s -axis, it is not clear but in linear scale one can see $\eta/s \propto \tau_c$ for non-interacting and $eB = 0$ case and its crossing point with KSS line has T -dependence - $\tau_c(T) = 5/(4\pi T)$. For interacting picture, still linear relation $\eta/s \propto \tau_c$ maintained but it get suppressed due to T -dependent interaction information, entered through $g(T)$, $E_{\text{av}}(T)$ etc. In presence of magnetic, quark component follow $\frac{\eta_1}{s} \propto \frac{\tau_c}{1+4(\tau_c/\tau_B)^2}$, for which a non-linear trend

Table 1: Order of magnitude of η/s from different model calculations (first column) with references at temperature range below (second column) and above (third column) transition temperature T_c .

Framework [Reference]	$T \leq T_c$	$T \geq T_c$
HTL [68]	-	1.8
NJL [69]	1-0.3	0.3-0.08
NJL [70]	1-0.5	0.5-0.55
NJL [71]	-	0.5-0.12
NJL [72]	2-0.25	0.25-0.5
LSM [73]	0.87-0.55	0.55-0.62
PQM [74]	5-0.5	0.3-0.08
URQMD [75]	1	-
SMASH [76]	1	-
EHL [78]	0.4-0.1	-
EHL [79]	0.8-0.25	-
HRG [80]	0.13-0.28	-
K-matrix HRG [81]	0.3-0.08	-
K-matrix HRG [82]	0.4-0.08	-

can be expected but gluon component remain same as without field case. So, when we add gluon and quark components, a mild non-linear nature is observed.

3.2 Merits, Demerits and Outlook

Present work has attempted to map LQCD thermodynamics in presence of magnetic field [5, 6] by using T , B dependent tuning parameters - degeneracy factor $g(T, B)$, average energy $E_{av}(T, B)$, momentum $k_{av}(T, B)$, velocity $v_{av}(T, B)$ of the constituents of QGP system. Now for massless (SB limit) and $B = 0$ case, their values are $g(T, B = 0) = 1$ (which is basically the maximum limit of the fraction, multiplied with total degeneracy factor 52 of QGP system), $E_{av}(T, B = 0) = k_{av}(T, B = 0) = 3T$ and $v_{av}(T, B = 0) = 1$. In presence of QCD interaction, $g(T, B = 0) < 1$, $E_{av}(T, B = 0) < 1$, $k_{av}(T, B = 0) < 3T$ and $v_{av}(T, B = 0) < 1$, which are observed during tuning these parameters to fit the LQCD data. When external magnetic field is applied to the interacting QCD system, the $g(T, B)$ face further suppression (in hadronic temperature range) and $E_{av}(T, B)$, $k_{av}(T, B)$ and $v_{av}(T, B)$ face enhancement with a non-monotonic T -profile. So this picture is quite simple and no quantum effect via Landau quantization has been considered, which might be the demerit part of the present model. Whereas simple picture with analytic type expression might be considered as the merit part of the model. Though the methodology is not so robust, but with the help of its simple parametric expressions, one can get a quick rough estimation of any phenomenological quantity, influenced by temperature and magnetic field dependent QCD interaction. For example, Feynman diagrams connected with QGP signal like strange enhancement, thermal dilepton and photon production, heavy quark diffusion, jet quenching parameters etc. might be calculated in quasi-particle kinematics and phase-space, which might provide us a non-perturbative estimations. However, actual quantitative calculations of different signal related phenomenology needs more details knowledge, which may be presented elsewhere.

4 Summary

The present article is first aimed to map the QCD interaction in a very simplified way. It is LQCD simulation, which has provided the QCD interaction at finite temperature and magnetic field by calculating thermodynamical quantities of QGP, which always remain lower than their non-interacting or massless values, popularly called SB limits. Along with the thermodynamics, LQCD calculation has found temperature and magnetic field dependent of quark condensate, which exposes inverse magnetic catalysis phenomenon near quark-hadron transition temperature. Constructing constituent quark mass, proportional to the temperature and magnetic field dependent quark condensate of LQCD, we have first obtained total number density of QGP, which is certainly deviated from its massless or SB limit. Assuming degeneracy factor as one of the tuning parameter, we have matched LQCD based total number density, which indirectly map the quark condensate of LQCD. Next, to match the LQCD thermodynamical quantities like pressure, energy density, entropy density, we have considered a temperature and magnetic field dependent average energy, momentum and velocity of partons (quarks/gluons) and tuned them accordingly.

After mapping temperature and magnetic field dependent of QCD interaction, we have applied it to calculate transport coefficients like shear viscosity and electrical conductivity in presence of magnetic field. Isotropic property of medium is generally broken due to magnetic field and hence, single component transport coefficient are splitted into multi-components, which can be classified into two main components - parallel and perpendicular components of transport coefficients. There can be Hall component at non-zero quark chemical potential but since here our focus on zero chemical potential zone, so net Hall component will be disappeared due to cancellation of quark and anti-quark contribution. Our final expressions of transport coefficients carry two time scales, originated from collision and magnetic field, where latter one Completely vanished at zero magnetic field case. So the differences among different component of transport coefficients are coming due to their different functional dependence with the magnetic time scale, which is basically inverse of synchrotron frequency of quarks. Qualitatively, we find a overall suppression of transport coefficient because of magnetic field and then when we plug in the LQCD interaction, they get further suppression. Based on the present study, one can identify the magnetic field and interaction as two dominating sources, for which the transport coefficients of QGP become lower. The well famous - low values shear viscosity to entropy density ratio might be linked with these two sources. This understanding might be better when a magneto-hydrodynamic simulation provide the values of shear viscosity to entropy density ratio by matching relevant experimental data.

Acknowledgment: SG and JD acknowledge to MHRD funding via IIT Bhilai and SS acknowledges to facilities, provided from IIT Bhilai in self-sponsor PhD scheme. AM and SP thank for (payment basis) hospitality from IIT Bhilai during his summer internship tenure (May-June, 2019).

5 Appendix

5.1 Shear viscosity calculation in presence of magnetic field

Let us consider a relativistic fermion/boson fluid, whose dissipative energy momentum tensor $\Delta T_{\mu\nu}$ due to shear stress is connected with velocity gradient-type tensor

$$\begin{aligned} U_{\mu\nu} &= D^\mu u^\nu + D^\nu u^\mu + \frac{2}{3} \Delta^{\mu\nu} \partial_\sigma u^\sigma \quad \text{with} \\ D^\mu &= \partial^\mu - u^\mu u^\sigma \partial_\sigma, \quad \Delta^{\mu\nu} = u^\mu u^\nu - g^{\mu\nu} . \end{aligned} \quad (32)$$

via macroscopic relation

$$\Delta T_{\mu\nu} = \eta_{\mu\nu\alpha\beta} U^{\alpha\beta}, \quad (33)$$

where $\eta_{\mu\nu\alpha\beta}$ is shear viscosity tensor, which is aimed to estimated microscopically in this section. Assuming fermion/boson equilibrium distribution function

$$f_0 = \frac{1}{e^{\beta\omega} \mp 1} \quad (34)$$

get deviation

$$\begin{aligned} \delta f &= -\phi \left(\frac{\partial f_0}{\partial \omega} \right) \\ &= -A(k_\mu k_\nu U^{\mu\nu}) \left(\frac{\partial f_0}{\partial \omega} \right) \\ &= A(k_\mu k_\nu U^{\mu\nu}) \beta f_0 (1 \mp f_0), \end{aligned} \quad (35)$$

we can get microscopic expression of (dissipative) energy-momentum

$$\begin{aligned} \Delta T_{\mu\nu} &= g \int \frac{d^3 \vec{k}}{(2\pi)^3} \frac{k_\mu k_\nu}{\omega} \delta f \\ &= g\beta \int \frac{d^3 \vec{k}}{(2\pi)^3} \frac{k_\mu k_\nu}{\omega} k_\alpha k_\beta U^{\alpha\beta} A f_0 (1 \mp f_0), \end{aligned} \quad (36)$$

where $\omega = \{k^2 + m^2\}^{1/2}$ is energy and g is degeneracy factor of fermion/boson. To determine unknown constant A , we use the relaxation time approximation (RTA) in Boltzmann equation,

$$\begin{aligned} \frac{\partial f}{\partial t} + \frac{\partial x^j}{\partial t} \frac{\partial f}{\partial x^j} + \frac{\partial k_j}{\partial t} \frac{\partial f}{\partial k^j} &= \mathcal{C}[\delta f] \\ \frac{\partial f}{\partial t} + \frac{k^j}{\omega} \frac{\partial f}{\partial x^j} &= \frac{\delta f}{\tau_c} \\ \Rightarrow \delta f &= \frac{\tau_c}{\omega} k^\mu \partial_\mu f_0 \text{ (since, } \frac{\partial k_j}{\partial t} = 0) \\ &= \frac{\tau_c}{\omega} k^\mu k^\nu U_{\mu\nu} \beta f_0 (1 \mp f_0) \end{aligned} \quad (37)$$

Comparing Eq. (37) and (35), one can identify the unknown constant

$$A = \frac{\tau_c}{\omega} \quad (38)$$

After knowing A , the full connection between macroscopic Eq. (33) and microscopic Eq. (36) can be written as

$$\begin{aligned} \eta_{\mu\nu\alpha\beta} U^{\alpha\beta} &= \Delta T^{\mu\nu} = g \int \frac{d^3 \vec{k}}{(2\pi)^3} \frac{k_\mu k_\nu}{\omega} \delta f \\ &= \left\{ g\beta \int \frac{d^3 \vec{k}}{(2\pi)^3} \frac{k_\mu k_\nu k_\alpha k_\beta}{\omega^2} \tau_c f_0 (1 \mp f_0) \right\} U^{\alpha\beta} \\ \Rightarrow \eta &= \frac{g\beta}{15} \int \frac{d^3 \vec{k}}{(2\pi)^3} \frac{k^4}{\omega^2} \tau_c f_0 (1 \mp f_0), \end{aligned} \quad (39)$$

where we have used the angular average (denoted by $\langle \dots \rangle_\theta$) identity

$$\langle k_\alpha k_\beta k_\gamma k_\delta \rangle_\theta = \frac{k^4}{15} (\delta_{\alpha\beta} \delta_{\gamma\delta} + \delta_{\alpha\gamma} \delta_{\beta\delta} + \delta_{\alpha\delta} \delta_{\beta\gamma}) . \quad (40)$$

The isotropic property of shear viscosity η does not hold in presence of magnetic field. Instead of single η , we will get many component η_n , which mean that different directional shear stress become different in presence of magnetic field. Following the prescriptions of Ref. [16, 20], the dissipative part of the energy-momentum tensor in presence of magnetic field B can be expressed as

$$\Delta T_{\alpha\beta} = \sum_{n=0}^4 \eta_n V_{\alpha\beta}^n \quad (41)$$

where η_n with $n = 0, 1, 2, 3, 4$ are five components of viscosities and the velocity gradient-type tensor $V_{\mu\nu}^n$ are taken same as addressed in Ref. [16, 17]:

$$V_{\alpha\beta}^0 = (3b_\alpha b_\beta - \delta_{\alpha\beta})(b_\gamma b_\delta V_{\gamma\delta} - \frac{\vec{\nabla} \cdot \vec{v}}{3}) \quad (42)$$

$$V_{\alpha\beta}^1 = 2V_{\alpha\beta} + \delta_{\alpha\beta} V_\gamma b_\gamma b_\delta - 2V_{\alpha\gamma} b_\gamma b_\beta - 2V_{\beta\gamma} b_\gamma b_\alpha (b_\alpha b_\beta - \delta_{\alpha\beta}) \vec{\nabla} \cdot \vec{v} + b_\alpha b_\beta V_{\alpha\delta} b_\gamma b_\delta \quad (43)$$

$$V_{\alpha\beta}^2 = 2(V_{\alpha\gamma} b_\beta b_\gamma + V_{\beta\gamma} b_\alpha b_\gamma - 2b_\alpha b_\beta V_{\gamma\delta} b_\gamma b_\delta) \quad (44)$$

$$V_{\alpha\beta}^3 = V_{\alpha\gamma} b_\beta b_\gamma + V_{\beta\gamma} b_\alpha b_\gamma - V_{\gamma\delta} b_{\alpha\gamma} b_\beta b_\delta - V_{\gamma\delta} b_{\beta\gamma} b_\alpha b_\delta \quad (45)$$

$$V_{\alpha\beta}^4 = 2(V_{\gamma\delta} b_{\alpha\gamma} b_\beta b_\delta + V_{\gamma\delta} b_{\beta\gamma} b_\alpha b_\delta) \quad (46)$$

with $b_\alpha = B_\alpha/B$, $b_{\alpha\beta} = \epsilon_{\alpha\beta\mu} B^\mu/B$, $V_{\alpha\beta} = \frac{1}{2} \left[\frac{\partial u_\alpha}{\partial x_\beta} + \frac{\partial u_\beta}{\partial x_\alpha} \right]$. Let us assume our deviation δf from equilibrium accordingly:

$$\begin{aligned} \delta f &= -\phi \left(\frac{\partial f_0}{\partial \omega} \right) \\ &= -\sum_{n=0}^4 A_n (k_\mu k_\nu U_n^{\mu\nu}) \left(\frac{\partial f_0}{\partial \omega} \right) \\ &= \sum_{n=0}^4 A_n (k_\mu k_\nu U_n^{\mu\nu}) \beta f_0 (1 \mp f_0) , \end{aligned} \quad (47)$$

To determine unknown constant A , we use the relaxation time approximation (RTA) in relativistic Boltzmann equation (RBE) at finite B ,

$$\begin{aligned} \frac{\partial f}{\partial t} + \frac{\partial x^j}{\partial t} \frac{\partial f}{\partial x^j} + \frac{\partial k_j}{\partial t} \frac{\partial f}{\partial k^j} &= \mathcal{C}[\delta f] \\ \frac{1}{\omega} k^\mu \partial_\mu f_0 + \frac{\tilde{e}B}{\omega} b_{\alpha\beta} k_\beta \frac{\partial(\delta f)}{\partial k_\alpha} &= \frac{\delta f}{\tau_c} , \end{aligned} \quad (48)$$

where force term in RBE can not contribute with f_0 , therefore, we have to proceed for δf order contribution. In other way, magnetic relaxation time $\tau_B = \omega/(\tilde{e}B)$ along with collisional relaxation time τ_c are responsible for deviation δf . Now, by using Eq. (47) in (48), we get

$$\frac{1}{\omega} k_\alpha k_\beta V_{\alpha\beta} \{ \beta f_0 (1 \mp f_0) \} + \frac{b_{\alpha\beta} k_\beta}{\tau_B} \left(\sum_{n=0}^4 A_n V_{\alpha\gamma}^n k_\gamma \right) \{ \beta f_0 (1 \mp f_0) \}$$

$$= -\frac{1}{\tau_c} \sum_{n=0}^4 A_n V_{\gamma\delta}^n k_\gamma k_\delta \{\beta f_0(1 \mp f_0)\} \quad (49)$$

Using some identities [16, 17, 20] and then compare the tensor structures on both sides to obtain A_n as follows

$$A_1 = \frac{\tau_c}{\omega} \frac{1}{4(1 + \frac{\tau_c^2}{\tau_B^2})} \quad (50)$$

$$A_2 = \frac{\tau_c}{\omega} \frac{1}{(1 + \frac{\tau_c^2}{\tau_B^2})} \quad (51)$$

$$A_3 = \frac{\tau_c}{\omega} \frac{(\frac{\tau_c}{\tau_B})}{2(1/4 + \frac{\tau_c^2}{\tau_B^2})} \quad (52)$$

$$A_4 = \frac{\tau_c}{\omega} \frac{(\frac{\tau_c}{\tau_B})}{(1 + \frac{\tau_c^2}{\tau_B^2})} \quad (53)$$

$$(54)$$

Putting the A_n 's in the expression for η_n we get

$$\eta_1 = \frac{g\beta}{15} \int \frac{d^3\vec{k}}{(2\pi)^3} \frac{\vec{k}^4}{\omega^2} \frac{\tau_c}{4(\frac{1}{4} + \frac{\tau_c^2}{\tau_B^2})} f_0(1 \mp f_0) \quad (55)$$

$$\eta_2 = \frac{g\beta}{15} \int \frac{d^3\vec{k}}{(2\pi)^3} \frac{\vec{k}^4}{\omega^2} \frac{\tau_c}{(1 + \frac{\tau_c^2}{\tau_B^2})} f_0(1 \mp f_0) \quad (56)$$

$$\eta_3 = \frac{g\beta}{15} \int \frac{d^3\vec{k}}{(2\pi)^3} \frac{\vec{k}^4}{\omega^2} \frac{\tau_c(\frac{\tau_c}{\tau_B})}{2(1/4 + \frac{\tau_c^2}{\tau_B^2})} f_0(1 \mp f_0) \quad (57)$$

$$\eta_4 = \frac{g\beta}{15} \int \frac{d^3\vec{k}}{(2\pi)^3} \frac{\vec{k}^4}{\omega^2} \frac{\tau_c(\frac{\tau_c}{\tau_B})}{(1 + \frac{\tau_c^2}{\tau_B^2})} f_0(1 \mp f_0) \quad (58)$$

$$(59)$$

One can identify parallel, perpendicular and Hall components as $\eta_{xzxz} = \eta_{\parallel} = \eta_2$, $\eta_{xyxy} = \eta_{\perp} = \eta_1$ and $\eta_{\times} = \eta_4$. If we take $B \rightarrow 0$ limit then η_{\parallel} and η_{\perp} will be merged to its isotropic value η and η_{\times} will be disappeared.

5.2 Electrical conductivity calculation in presence of magnetic field

Let us consider a relativistic fermion/boson fluid, carrying dissipative current density J_i due to electric field E^j and they are connected via macroscopic Ohm's law

$$J_i = \sigma_{ij} E^j, \quad (60)$$

where σ_{ij} is conductivity tensor, which is aimed to estimated microscopically in this section. Assuming fermion/boson equilibrium distribution function

$$f_0 = \frac{1}{e^{\beta\omega} \mp 1} \quad (61)$$

get deviation

$$\begin{aligned}
\delta f &= -\phi\left(\frac{\partial f_0}{\partial \omega}\right) \\
&= -\alpha(k_j E^j)\left(\frac{\partial f_0}{\partial \omega}\right) \\
&= \alpha(k_j E^j)\beta f_0(1 \mp f_0) ,
\end{aligned} \tag{62}$$

we can get microscopic expression of (dissipative) current density

$$\begin{aligned}
J_i &= g\tilde{e} \int \frac{d^3 \vec{k}}{(2\pi)^3} \frac{k_i}{\omega} \delta f \\
&= g\tilde{e}\beta \int \frac{d^3 \vec{k}}{(2\pi)^3} \frac{k_i k_j}{\omega} \alpha f_0(1 \mp f_0) ,
\end{aligned} \tag{63}$$

where \tilde{e} is electric charge, $\omega = \{\vec{k}^2 + m^2\}^{1/2}$ is energy and g is degeneracy factor (excluding charge-flavor degeneracy) of fermion/boson. To determine unknown constant α , we use the Boltzmann equation,

$$\frac{\partial f}{\partial t} + \frac{\partial x^j}{\partial t} \frac{\partial f}{\partial x^j} + \frac{dk_j}{dt} \frac{\partial f}{\partial k^j} = \mathcal{C}[\delta f] . \tag{64}$$

In the electric-charge-transport picture, the external electric field is responsible to make the system deviate from equilibrium. Hence electric force $-\tilde{e}E_j = \frac{dk_j}{dt}$ will build the deviation δf and in relaxation time approximation (RTA), we may assume $\mathcal{C}[\delta f] = -\delta f/\tau_c$, where τ_c is the relaxation time, required for the system to approach from non-equilibrium to equilibrium state. So, Eq. (64) becomes

$$\begin{aligned}
-\tilde{e}E_j \frac{\partial f_0}{\partial k^j} &= -\delta f/\tau_c \\
\Rightarrow \delta f &= \tau_c \tilde{e} E_j \left(\frac{\partial \omega}{\partial k^j}\right) \left[\frac{\partial f_0}{\partial \omega}\right] \\
&= \tau_c \tilde{e} E_j \left(\frac{k^j}{\omega}\right) [\beta f_0(1 \mp f_0)]
\end{aligned} \tag{65}$$

comparing Eq. (65) and (62), one can identify the unknown constant

$$\alpha = \frac{\tilde{e}\tau_c}{\omega} \tag{66}$$

After knowing α , the full connection between macroscopic Eq. (60) and microscopic Eq. (63) can be written as

$$\begin{aligned}
\sigma^{ij} E_j &= J_D^i = g\tilde{e} \int \frac{d^3 \vec{k}}{(2\pi)^3} \frac{k^i}{\omega} \delta f \\
&= \left\{ g\tilde{e}^2 \beta \int \frac{d^3 \vec{k}}{(2\pi)^3} \frac{k^i k^j}{\omega^2} \tau_c f_0(1 \mp f_0) \right\} E_j \\
\Rightarrow \sigma^{ij} &= g\tilde{e}^2 \beta \int \frac{d^3 \vec{k}}{(2\pi)^3} \tau_c \frac{k^i k^j}{\omega^2} f_0(1 \mp f_0) \\
\Rightarrow \sigma &= \frac{1}{3} g\tilde{e}^2 \beta \int \frac{d^3 \vec{k}}{(2\pi)^3} \tau_c \frac{\vec{k}^2}{\omega^2} f_0(1 \mp f_0) .
\end{aligned} \tag{67}$$

Next, we will proceed to derive the electrical conductivity in presence of magnetic field B , which is well addressed in Ref. [27]. Here, force term becomes $\frac{d\vec{k}}{dt} = -\tilde{e}(\vec{E} + \vec{v} \times \vec{B})$ and so, the Boltzmann equation (64) becomes

$$\begin{aligned} -\tilde{e}(\vec{E} + \frac{\vec{k}}{\omega} \times \vec{B}) \cdot \nabla_k f_0 &= \mathcal{C}[\delta f] \\ -\tilde{e}(\vec{E} + \frac{\vec{k}}{\omega} \times \vec{B}) \cdot \left(\frac{\vec{k}}{\omega}\right) \frac{\partial f_0}{\partial \omega} &= \frac{-\delta f}{\tau_c}. \end{aligned} \quad (68)$$

Since the second term of left had side is only magnetic field dependent term and it will be vanished (following vector identity $(\vec{k} \times \vec{B}) \cdot \vec{k} = \vec{B} \cdot (\vec{k} \times \vec{k}) = 0$), so we consider the $\nabla_k(\delta f)$ term also

$$-\tilde{e}\vec{E} \cdot \left(\frac{\vec{k}}{\omega}\right) \frac{\partial f_0}{\partial \omega} - \tilde{e}\left(\frac{\vec{k}}{\omega} \times \vec{B}\right) \cdot \nabla_k(\delta f) = -\delta f/\tau_c, \quad (69)$$

where we assume $\delta f = -\phi \frac{\partial f_0}{\partial \omega}$ with $\phi = \vec{k} \cdot \vec{F}$ and $\vec{F} = (\alpha \hat{e} + \beta \hat{h} + \gamma(\hat{e} \times \hat{h}))$, \hat{e} and \hat{h} are unit vector along electric and magnetic field directions. Since

$$\begin{aligned} \left(\frac{\vec{k}}{\omega} \times \vec{B}\right) \cdot \nabla_k(\delta f) &= -\left(\frac{\vec{k}}{\omega} \times \vec{B}\right) \cdot \nabla_k(\vec{k} \cdot \vec{F}) \frac{\partial f_0}{\partial \omega} \\ &= -\left(\frac{\vec{k}}{\omega} \times \vec{B}\right) \cdot \vec{F} \frac{\partial f_0}{\partial \omega} \\ &= -\frac{\vec{k}}{\omega} \cdot (\vec{B} \times \vec{F}) \frac{\partial f_0}{\partial \omega}, \end{aligned} \quad (70)$$

so Eq. (69) becomes

$$\begin{aligned} \left(\frac{\vec{k}}{\omega}\right) \cdot \left[-\tilde{e}\vec{E} + \tilde{e}(\vec{B} \times \vec{F})\right] &= \vec{k} \cdot \vec{F}/\tau_c, \\ \frac{1}{\omega} \left[-\tilde{e}E\hat{e} + \tilde{e}B\hat{h} \times (\alpha\hat{e} + \beta\hat{h} + \gamma(\hat{e} \times \hat{h}))\right] &= (\alpha\hat{e} + \beta\hat{h} + \gamma(\hat{e} \times \hat{h}))/\tau_c \\ \left(-\frac{\tau_c \tilde{e}E}{\omega}\right)\hat{e} - \left(\frac{\tau_c \tilde{e}B\alpha}{\omega}\right)(\hat{e} \times \hat{h}) + \left(\frac{\tau_c \tilde{e}B\gamma}{\omega}\right)\{\hat{e} - (\hat{e} \cdot \hat{h})\hat{h}\} &= (\alpha\hat{e} + \beta\hat{h} + \gamma(\hat{e} \times \hat{h})) \end{aligned} \quad (71)$$

Equating the coefficients of \hat{e} , \hat{h} and $(\hat{e} \times \hat{h})$ of Eq. (71), we get

$$\begin{aligned} \left(\frac{-\tau_c \tilde{e}E}{\omega} + \frac{\tau_c \gamma}{\tau_B}\right) &= \alpha \\ \left(\frac{\tau_c \gamma}{\tau_B}\right)(\hat{e} \cdot \hat{h}) &= \beta \\ -\left(\frac{\tau_c \alpha}{\tau_B}\right) &= \gamma, \end{aligned} \quad (72)$$

where $\tau_B = \omega/(eB)$ is inverse of synchrotron frequency. Solving them, we get

$$\begin{aligned} \alpha &= \left(\frac{-\tilde{e}E\tau_c}{\omega}\right) \frac{1}{1 + (\tau_c/\tau_B)^2} \\ \beta &= (\hat{e} \cdot \hat{h})(\tau_c/\tau_B)^2 \alpha = \left(\frac{-\tilde{e}E\tau_c}{\omega}\right) (\hat{e} \cdot \hat{h}) \frac{(\tau_c/\tau_B)^2}{1 + (\tau_c/\tau_B)^2} \\ \gamma &= (-\tau_c/\tau_B)\alpha = \left(\frac{\tilde{e}E\tau_c}{\omega}\right) \frac{(\tau_c/\tau_B)}{1 + (\tau_c/\tau_B)^2}. \end{aligned} \quad (73)$$

In terms of these coefficients, now we can write

$$\phi = \frac{e\tau_c}{1 + (\tau_c/\tau_B)^2} \frac{k_i}{\omega} \{\delta_{ij} - (\tau_c/\tau_B)\epsilon_{ijk}h_k + (\tau_c/\tau_B)^2 h_i h_j\} E^j . \quad (74)$$

Now, the connection between Eqs. (60) and (63) becomes

$$\begin{aligned} \sigma^{ij} E_j &= J_D^i \\ &= g\tilde{e} \int \frac{d^3\vec{k}}{(2\pi)^3} \frac{k^i}{\omega} \delta f \\ &= g\tilde{e}\beta \int \frac{d^3\vec{k}}{(2\pi)^3} \frac{k^i}{\omega} \phi f_0 (1 \mp f_0) , \quad [\text{since } \delta f = -\phi \frac{\partial f_0}{\partial \omega} = \phi \beta f_0 (1 \mp f_0)] \\ \Rightarrow \sigma^{ij} &= \delta^{ij} \sigma_0 - \epsilon^{ijk} h_k \sigma_1 + h^i h^j \sigma_2 , \end{aligned} \quad (75)$$

where

$$\sigma_n = g\tilde{e}^2 \frac{\beta}{3} \int \frac{d^3\vec{k}}{(2\pi)^3} \tau \frac{\vec{k}^2}{\omega^2} \frac{\tau_c (\tau_c/\tau_B)^n}{1 + (\tau_c/\tau_B)^2} f_0 (1 \mp f_0) . \quad (76)$$

If we consider \hat{h} in z direction, then conductivity matrix elements will be $\sigma^{xx} = \sigma^{yy} = \sigma_0$, $\sigma^{xy} = -\sigma^{yx} = -\sigma_1$, $\sigma^{zz} = \sigma_0 + \sigma_2$ and remaining are zero. We can use other notations $\sigma_{\parallel} = \sigma_{zz}$, $\sigma_{\perp} = \sigma_{xx}$, $\sigma_{\times} = \sigma_{xy}$, which represents parallel, perpendicular and Hall component in more distinctly.

References

- [1] T.Vachaspati, *Magnetic fields from cosmological phase transitions*, Phys. Lett. **B** 265 (1991) 258–261.
- [2] R. C. Duncan and C. Thompson, *Formation of Very Strongly Magnetized Neutron Stars: Implications for Gamma-Ray Bursts*, Astrophys. J. **392** (1992) L9.
- [3] I. A. Shovkovy, Lect. Notes Phys. **871**, 13 (2013), arXiv:1207.5081 [hep-ph].
- [4] Kenji Fukushima, Dmitri E. Kharzeev, Harmen J. Warringa, *Chiral magnetic effect*, Phys. Rev. **D** **78** 074033 (2008), [arXiv:0808.3382 [hep-ph]]
- [5] G.S. Bali, F. Bruckmann, G. Endrodi, Z. Fodor, S.D. Katz, and A. Schafer, *QCD quark condensate in external magnetic fields*, Phys. Rev. **D** **86**, 071502(R), 2012.
- [6] G.S. Bali, F. Bruckmann, G. Endrodi, S.D. Katz, A. Schafer, *The QCD equation of state in background magnetic fields* J. High Energ. Phys. 1408 (2014) 177.
- [7] K. Tuchin, *Particle production in strong electromagnetic fields in relativistic heavy-ion collisions*, Adv. High Energy Phys. **2013**, 490495 (2013) doi:10.1155/2013/490495 [arXiv:1301.0099 [hep-ph]].
- [8] W. T. Deng and X. G. Huang, *Event-by-event generation of electromagnetic fields in heavy-ion collisions*, Phys. Rev. C **85**, 044907 (2012) doi:10.1103/PhysRevC.85.044907 [arXiv:1201.5108 [nucl-th]].
- [9] D. Satow, *Nonlinear electromagnetic response in quark-gluon plasma*, Phys. Rev. D **90**, no. 3, 034018 (2014) doi:10.1103/PhysRevD.90.034018 [arXiv:1406.7032 [hep-ph]].

- [10] V. Skokov, A. Illarionov and V. Toneev, *ESTIMATE OF THE MAGNETIC FIELD STRENGTH IN HEAVY-ION COLLISIONS*, Int. J. Mod. Phys. **A 24**, 5925 (2009)
- [11] V. Roy, S. Pu, L. Rezzolla and D. Rischke, *Analytic Bjorken flow in one-dimensional relativistic magnetohydrodynamics*, Phys. Lett. B **750**, 45 (2015) doi:10.1016/j.physletb.2015.08.046 [arXiv:1506.06620 [nucl-th]].
- [12] S. Pu, V. Roy, L. Rezzolla and D. H. Rischke, *Bjorken flow in one-dimensional relativistic magnetohydrodynamics with magnetization*, Phys. Rev. D **93**, no. 7, 074022 (2016) doi:10.1103/PhysRevD.93.074022 [arXiv:1602.04953 [nucl-th]].
- [13] M. Hongo, Y. Hirono and T. Hirano, *Anomalous-hydrodynamic analysis of charge-dependent elliptic flow in heavy-ion collisions*, arXiv:1309.2823 [nucl-th].
- [14] G. Inghirami, L. Del Zanna, A. Beraudo, M. H. Moghaddam, F. Becattini and M. Bleicher, *Numerical magneto-hydrodynamics for relativistic nuclear collisions*, Eur. Phys. J. C **76**, no. 12, 659 (2016) doi:10.1140/epjc/s10052-016-4516-8 [arXiv:1609.03042 [hep-ph]].
- [15] S. K. Das, S. Plumari, S. Chatterjee, J. Alam, F. Scardina and V. Greco, *Directed Flow of Charm Quarks as a Witness of the Initial Strong Magnetic Field in Ultra-Relativistic Heavy Ion Collisions*, Phys. Lett. B **768**, 260 (2017) doi:10.1016/j.physletb.2017.02.046 [arXiv:1608.02231 [nucl-th]].
- [16] E.M. Lifshitz and L.P. Pitaevskii, 1987 *Physical kinetics*, Pergamon Press, U.K.
- [17] K. Tuchin, *On viscous flow and azimuthal anisotropy of the quark-gluon plasma in a strong magnetic field* J. Phys. G: Nucl. Part. Phys. **39** (2012) 025010.
- [18] S. Li, H-U Yee, *Shear Viscosity of Quark-Gluon Plasma in Weak Magnetic Field in Perturbative QCD: Leading Log* Phys. Rev. **D 97**, 056024 (2018).
- [19] P. Mohanty, A. Dash, V. Roy, *One particle distribution function and shear viscosity in magnetic field: A relaxation time approach*, Eur. Phys. J. **A 55** (2019) 35.
- [20] J Dey, S. Satapathy, P. Murmu, S. Ghosh *Shear viscosity and electrical conductivity of relativistic fluid in presence of magnetic field: a massless case*, arXiv:1907.11164 [hep-ph].
- [21] S. Ghosh, B. Chatterjee, P. Mohanty, A. Mukharjee, H. Mishra *Impact of magnetic field on shear viscosity of quark matter in Nambu-Jona-Lasinio model*, Phys. Rev. **D 100** (2019) 034024.
- [22] S. Nam and C-W Kao, *Shear viscosity of quark matter at finite temperature under an external magnetic field*, Phys. Rev. **D 87**, 114003 (2013).
- [23] A. Dash, S. Samanta, J. Dey, U. Gangopadhyaya, S. Ghosh, V. Roy, *Anisotropic transport properties of Hadron Resonance Gas in magnetic field*, arxiv: 2002.08781 [nucl-th]
- [24] Z. Chen, C. Greiner, A. Huang, Z. Xu, *Calculation of anisotropic transport coefficients for an ultrarelativistic Boltzmann gas in a magnetic field within a kinetic approach*, Phys. Rev. D **101** (2020) 056020.
- [25] A. Das, H. Mishra, R. K. Mohapatra, *Transport coefficients of hot and dense hadron gas in a magnetic field: a relaxation time approach* Phys. Rev. **D 100** (2019) 114004.

- [26] G. S. Denicol, X. G. Huang, E. Molnár, G. M. Monteiro, H. Niemi, J. Noronha, D. H. Rischke, and Q. Wang, *Nonresistive dissipative magnetohydrodynamics from the Boltzmann equation in the 14-moment approximation*, Phys. Rev. D **98**, 076009 (2018).
- [27] A. Harutyunyan and A. Sedrakian, *Electrical conductivity of a warm neutron star crust in magnetic fields*, Phys. Rev. C **94**, no. 2, 025805 (2016) doi:10.1103/PhysRevC.94.025805 [arXiv:1605.07612 [astro-ph.HE]].
- [28] B. O. Kerbikov and M. A. Andreichikov, *Electrical Conductivity of Dense Quark Matter with Fluctuations and Magnetic Field Included*, Phys. Rev. D **91**, no. 7, 074010 (2015) doi:10.1103/PhysRevD.91.074010 [arXiv:1410.3413 [hep-ph]].
- [29] S. i. Nam, *Electrical conductivity of quark matter at finite T under external magnetic field*, Phys. Rev. D **86**, 033014 (2012) doi:10.1103/PhysRevD.86.033014 [arXiv:1207.3172 [hep-ph]].
- [30] X. G. Huang, A. Sedrakian and D. H. Rischke, *Kubo formulae for relativistic fluids in strong magnetic fields*, Annals Phys. **326**, 3075 (2011) doi:10.1016/j.aop.2011.08.001 [arXiv:1108.0602 [astro-ph.HE]].
- [31] K. Hattori, S. Li, D. Satow and H. U. Yee, *Longitudinal Conductivity in Strong Magnetic Field in Perturbative QCD: Complete Leading Order*, Phys. Rev. D **95**, no. 7, 076008 (2017) doi:10.1103/PhysRevD.95.076008 [arXiv:1610.06839 [hep-ph]].
- [32] M. Kurian, S. Mitra, S. Ghosh, V. Chandra, *Transport coefficients of hot magnetized QCD matter beyond the lowest Landau level approximation* Eur. Phys. J. C **79** (2019) 134.
- [33] M. Kurian, V. Chandra, *Effective description of hot QCD medium in strong magnetic field and longitudinal conductivity* Phys. Rev. D **96** (2017) 114026.
- [34] B. Feng, *Electric conductivity and Hall conductivity of the QGP in a magnetic field* Phys. Rev. D **96**, 036009 (2017).
- [35] K. Fukushima, Y. Hidaka, *Electric conductivity of hot and dense quark matter in a magnetic field with Landau level resummation via kinetic equations* Phys. Rev. Lett. **120**, 162301 (2018).
- [36] A. Das, H. Mishra, R. K. Mohapatra, *Electrical conductivity and Hall conductivity of a hot and dense hadron gas in a magnetic field: A relaxation time approach* Phys. Rev. D **99** (2019) 094031.
- [37] A. Das, H. Mishra, R. K. Mohapatra *Electrical conductivity and Hall conductivity of hot and dense quark gluon plasma in a magnetic field: a quasi particle approach*, Phys. Rev. D **101** (2020) 034027.
- [38] S. Ghosh, A. Bandyopadhyay, R.L.S. Farias, J. Dey, G. Krein, *NJL model estimation of anisotropic electrical conductivity for quark matter in presence of magnetic field*, arXiv: 1911.10005 [hep-ph].
- [39] S. Rath, B. K. Patra, *Revisit to electrical and thermal conductivities, Lorenz and Knudsen numbers in thermal QCD in a strong magnetic field*, Phys. Rev. D **100** (2019) 016009; *Effect of magnetic field on the charge and thermal transport properties of hot and dense QCD matter*, arXiv: 2005.00997 [hep-ph].

- [40] L. Thakur, P.K. Srivastava, *Electrical conductivity of a hot and dense QGP medium in a magnetic field* Phys. Rev. **D 100** (2019) 076016.
- [41] B. Chatterjee, R. Rath, G. Sarwar, R. Sahoo, *Centrality dependence of Electrical and Hall conductivity at RHIC and LHC energies for a Quark-Gluon Plasma Phase* arXiv: 1908.01121 [hep-ph].
- [42] M. Kurian, *Thermal transport in a weakly magnetized hot QCD medium*, arXiv:2005.04247 [nucl-th].
- [43] S. Samanta, J. Dey, S. Satapathy, S Ghosh, *Quantum expression of electrical conductivity from massless quark matter to hadron resonance gas in presence of magnetic field*, arXiv: 2002.04434 [nucl-th]
- [44] K. Hattori, X. G. Huang, D. H. Rischke and D. Satow, *Bulk Viscosity of Quark-Gluon Plasma in Strong Magnetic Fields* arXiv:1708.00515 [hep-ph].
- [45] X-G Huang, M. Huang, D. H. Rischke, A. Sedrakian, *Anisotropic hydrodynamics, bulk viscosities, and r -modes of strange quark stars with strong magnetic fields* Phys. Rev. **D 81**, 045015 (2010).
- [46] N.O. Agasian, *Bulk viscosity of quark-gluon matter in a magnetic field*, Phys. Atom. Nucl. 76 (2013) 1382.
- [47] N.O. Agasian, *Low-energy theorems of QCD and bulk viscosity at finite temperature and baryon density in a magnetic field*, JETP Lett. 95 (2012) 171.
- [48] M. Kurian, V. Chandra, *Bulk viscosity of a hot QCD medium in a strong magnetic field within the relaxation-time approximation* Phys. Rev. **D 97** (2018) 116008.
- [49] M. Kurian, S. K. Das, V. Chandra *Heavy quark dynamics in a hot magnetized QCD medium* arXiv:1907.09556 [nucl-th].
- [50] B. Singh, L. Thakur, H. Mishra *Heavy quark complex potential in a strongly magnetized hot QGP medium* Phys. Rev. **D 97** (2018) 096011.
- [51] Mark I. Gorenstein, Shin Nan Yang, *Gluon plasma with a medium-dependent dispersion relation*, Phys. Rev. **D 52**, 5206 (1995).
- [52] A.Peshier, B.Kampfer, O.P. Pavlenko, G. Soff, *Massive quasiparticle model of the $SU(3)$ gluon plasma* Phys. Rev. **D 54** (1996)
- [53] P. Levai and U. W. Heinz, *Massive gluons and quarks and the equation of state obtained from $SU(3)$ lattice QCD* Phys. Rev. C 57, 1879 (1998).
- [54] M. Bluhm, B. Kämpfer, and G. Soff, *The QCD equation of state near T_c within a quasi-particle model* Phys. Lett. B 620, 131 (2005).
- [55] V.M. Bannur, *Self-consistent quasiparticle model for quark-gluon plasma* Phys. Rev. **C 75**, 044905 (2007).
- [56] Salvatore Plumari, Wanda M. Alberico, Vincenzo Greco, Claudia Ratti, *Recent thermodynamic results from lattice QCD analyzed within a quasiparticle model* Phys. Rev. **84**, 094004 (2011).

- [57] P. N. Meisinger, M. C. Ogilvie, and T. R. Miller, *Gluon Quasiparticles and the Polyakov Loop* Phys. Lett. B 585, 149 (2004).
- [58] M. Ruggieri, P. Alba, P. Castorina, S. Plumari, C. Ratti, V. Greco, *Polyakov loop and gluon quasiparticles in Yang-Mills thermodynamics* Phys. Rev. D **86**, 054007 (2012).
- [59] V. Chandra, R. Kumar, V. Ravishankar, *Hot QCD equations of state and relativistic heavy ion collisions* Phys. Rev. C **76** (2007) 054909.
- [60] Vinod Chandra, V. Ravishankar, *Quasi-particle model for lattice QCD: Quark-gluon plasma in heavy ion collisions*, Eur. Phys. J. C **64** (2009) 63.
- [61] V. Chandra, V. Ravishankar, *A quasi-particle description of (2+1)- flavor lattice QCD equation of state* Phys. Rev. D **84**, 074013 (2011).
- [62] X. Li, W. Fu, Y. Liu, *Thermodynamics of 2+1 Flavor Polyakov-Loop Quark-Meson Model under External Magnetic Field* Phys. Rev. D **99** (2019) 074029.
- [63] A.N. Tawfik, A.M. Diab, M.T. Hussein, *Quark-hadron phase structure, thermodynamics, and magnetization of QCD matter* J. Phys. G 45 (2018) 055008.
- [64] A.N. Tawfik, A.M. Diab, N. Ezzelarab, A.G. Shalaby, *QCD thermodynamics and magnetization in nonzero magnetic field* Adv. High Energy Phys. 2016 (2016) 1381479.
- [65] R.L.S. Farias, V.S. Timoteo, S.S. Avancini, M.B. Pinto, G. Krein, *Thermo-magnetic effects in quark matter: Nambu-Jona-Lasinio model constrained by lattice QCD* Eur. Phys. J. A 53 (2017) 101.
- [66] S. Satapathy, S. Paul, A. Anand, R. Kumar, S. Ghosh, *From Non-interacting to Interacting Picture of Thermodynamics and Transport Coefficients for Quark Gluon Plasma* J. Phys. G **47** (2020) 045201.
- [67] P. Kovtun, D.T. Son, A.O. Starinets, *Viscosity in Strongly Interacting Quantum Field Theories from Black Hole Physics*, Phys. Rev. Lett. 94 (2005) 111601.
- [68] P. B. Arnold, G. D. Moore, and L. G. Yaffe, J. High Energy Phys. 11 (2000) 001.
- [69] R. Marty, E. Bratkovskaya, W. Cassing, J. Aichelin, and H. Berrehrach, Phys. Rev. C **88**, 045204 (2013).
- [70] C. Sasaki and K. Redlich, Nucl.Phys. A **832** (2010) 62.
- [71] S. Ghosh, T. C. Peixoto, V. Roy, F. E. Serna, G. Krein, Phys. Rev. C **93** (2016) 045205.
- [72] P. Deb, G. Kadam, H. Mishra, Phys. Rev. D **94** (2016) 094002.
- [73] P. Chakraborty and J. I. Kapusta, Phys. Rev. C **83**, 014906 (2011).
- [74] P. Singha, A. Abhishek, G. Kadam, S. Ghosh, H. Mishra, J. Phys. G 46 (2019) 015201.
- [75] N. Demir and S.A. Bass, Phys. Rev. Lett. 102, 172302 (2009).
- [76] J.-B. Rose, J. M. Torres-Rincon, A. Schäfer, D. R. Oliinychenko and H. Petersen, Phys. Rev. C 97, no. 5, 055204 (2018).

- [77] D. Fernandez-Fraile and A. Gomez Nicola, Eur. Phys. J. C **62**, 37 (2009).
- [78] S. Ghosh, G. Krein, S. Sarkar Phys. Rev. C89 (2014) 045201; S. Ghosh, Phys. Rev. C90 (2014) 025202; Braz. J. Phys. 45 (2015) 687; M. Rahaman, S. Ghosh, S. Ghosh, S. Sarkar, J. Alam, Phys. Rev. C 97 (2018) 035201.
- [79] P. Kalikotaya, N. Chaudhuri, S. Ghosh, U. Gangopadhyayab, S. Sarkar arXiv:1908.02933 [nucl-th].
- [80] S. Ghosh, S. Samanta, S. Ghosh, H. Mishra, Int. J. Mod. Phys. E 28 (2019) 1950036; S. Ghosh, S. Ghosh, S. Bhattacharyya, Phys. Rev. C 98 (2018) 045202
- [81] A Dash, S. Samanta, B. Mohanty, Phys. Rev. **D 100**, 014025 (2019).
- [82] G. Kadam, S. Pawar, H. Mishra, J. Phys. G 46 (2019) 015102.